Compact microwave re-entrant cavity applicator for plasma-assisted combustion

Kadek W. Hemawan,[1] Indrek S. Wichman,[2] Tonghun Lee,[2] Timothy A. Grotjohn,[1,3] and Jes Asmussen[1,3]
[1]*Department of Electrical and Computer Engineering, Michigan State University, East Lansing, Michigan 48824, USA*
[2]*Department of Mechanical Engineering, Michigan State University, East Lansing, Michigan 48824, USA*
[3]*Center for Coatings and Laser Applications, Fraunhofer USA, East Lansing, Michigan 48824, USA*

(Received 26 February 2009; accepted 18 April 2009; published online 20 May 2009)

The design and experimental operation of a compact microwave/rf applicator is described. This applicator operates at atmospheric pressure and couples electromagnetic energy into a premixed CH_4/O_2 flame. The addition of only 2–15 W of microwave power to a premixed combustion flame with a flame power of 10–40 W serves to extend the flammability limits for fuel lean conditions, increases the flame length and intensity, and increases the number density and mixture of excited radical species in the flame vicinity. The downstream gas temperature also increases. Optical emission spectroscopy measurements show gas rotational temperatures in the range of 2500–3600 K. At the higher input power of $\geq$10 W microplasma discharges can be produced in the high electric field region of the applicator. © *2009 American Institute of Physics.*
[DOI: 10.1063/1.3131623]

I. INTRODUCTION

In the past, many researchers have investigated techniques that combine electrical energy with a flame. They demonstrated the potential to modify the combustion process with the addition of electric energy. dc and ac discharges, dielectric barrier discharges (DBDs), rf discharges, pulsed corona discharges, plasmatrons, and microwave discharges were experimentally investigated for their ability to interact with and modify premixed and diffusion flames.

In particular, it was found that by impressing an electric field or high voltage into the flame, the flame stability limits were extended, the flame propagation speed was increased, and the flame chemistry[1,2] was altered. As observed by various research groups, the creation of reactive radicals or hydrogen generation resulted in combustion enhancement. Studies of hydrocarbon-air and carbon monoxide-air premixed flames in rf discharge plasmas demonstrated that large fractions of the fuels are burned in rf plasma generated flames.[3] A dc plasmatron was used for the pretreatment of the fuel to improve the combustion process and the conversion of methane to hydrogen.[4] In the DBD, the plasma power increased the flame propagation rate, resulting in a faster burn rate. The DBD has been usually used to investigate the efficiency of the combustion process. Leaner burning conditions can result when the flame is subjected to the nonthermal plasma discharge.[5–7] In ignition, the combustion processes are typically initiated by high temperature air or spark discharges that cause the thermal decomposition of the fuels into various highly reactive radical species. The utilization of transient plasma during the formation phase of pulse-ignited atmospheric discharges in a pulse detonation engine confirmed that the transient plasma produces shorter ignition delay times and pressure rise times compared to spark ignition.[8] This leads to cleaner combustion.

Microwave plasma-assisted hydrocarbon treatment was initially investigated for internal combustion engine improvement[9–13] and for the conversion of hydrocarbons into methane and acetylene gases.[14] More recently the conversion of hydrocarbons into hydrogen fuels has been investigated.[15] The application of microwave energy has been shown to assist ignition and flame holding, flame speed enhancement, and flame extinction limits.[16,17] The experiments of Zaidi *et al.*[17] demonstrated that microwave flame interaction was greatly enhanced with the use of a high Q microwave cavity applicator.

Recently we developed an experimental microwave system that enabled the repeatable controlled coupling of microwave energy into a premixed flame.[18] Microwave energy was coupled into a flame that was located inside a high Q, tunable 17.8 cm diameter cylindrical microwave cavity applicator. The idea of employing a tunable cavity applicator to impress, focus, and match microwave energy into a load has been applied earlier to material heating[19] and to a variety of microwave plasma source[20–26] applications. This method of microwave coupling and matching has been shown to be an efficient and controllable method for coupling microwave energy into dynamically varying loads such as microwave plasmas and microwave heated material loads. Indeed, our initial experimental results[18] demonstrated that microwave energy could be efficiently coupled into a combustion flame that was placed inside a tunable microwave cavity. However this microwave applicator system was physically large, and therefore additional improvements were desirable. In particu-

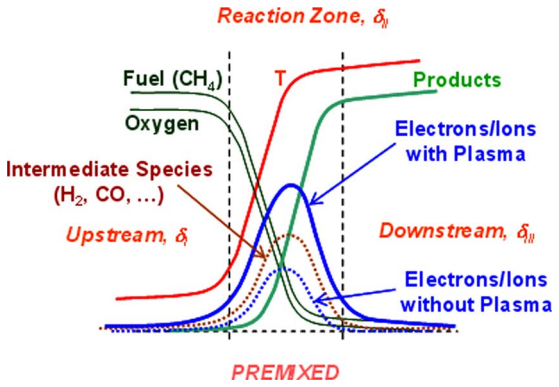

FIG. 1. (Color online) Combined thermal oxidation and plasma in a premixed flame adapted from Ref. 31. Radicals are formed in δ_I, they oxidize reactants and form intermediates (such as CO and H_2) in δ_{II}, and final products (such as CO_2 and H_2O) are formed in δ_{III}.

lar a reduction in the applicator size and a further improvement in the microwave coupling efficiency were desirable.

In this paper we describe an improved experimental microwave plasma-assisted combustion apparatus, which employs a more efficient and more compact microwave applicator that positions the flame in a region of high microwave electric field strength. The applicator consists of a tunable re-entrant coaxial cavity[20] that has been modified to allow the combustion flame to be excited in a small ($\leq$2 mm) variable gap located in a high electric field region of the applicator. The impressed electric field modifies the combustion process by coupling energy into the electron gas that, as shown in Fig. 1, exists even when no plasma is present. The addition of microwave energy increases the electron temperature and also through ionizing collisions increases the electron density. This electron gas is shown with and without the application of microwave energy in Fig. 1. Finally, as the impressed microwave electric field is additionally increased microplasma, microwave discharges can be produced in the gap region, further modifying the combustion process. These microwave microplasmas have the interesting potential of producing nonlocal thermal equilibrium plasmas at atmospheric pressure.[27,28] The description of the applicator and its initial exploratory performance are presented below.

II. EXPERIMENTAL SYSTEMS

A. The coaxial applicator

Figure 2 displays the microwave re-entrant cavity applicator placed adjacent to a 1 in. diameter silicon wafer, and Fig. 3 shows the microwave applicator exciting a combustion flame. The cylindrical applicator has a 3.5 cm diameter and length of 12 cm. As shown in Fig. 3, the microwave excited flame extends through a circular hole at the end of the applicator. Thus, the flame reaction zone can be observed outside the applicator. Microwave coupling occurs in a variable gap L_g located at the open end of the applicator.

FIG. 2. (Color) Photograph of the overall microwave re-entrant cavity applicator adjacent to a 1 in. silicon wafer.

FIG. 3. (Color) Photograph of the re-entrant cavity showing the microwave applicator exciting a premixed flame.

Figure 4 displays a cross-sectional view of the cylindrical cavity applicator. The applicator is a short-gap, re-entrant brass cavity excited in the transverse electromagnetic (TEM) mode[20] with three continuously variable tuning lengths: (1) a variable short length L_s, (2) a variable coupling loop position L_p, and (3) a variable gap L_g. The electromagnetic excitation region consists of an outer cylinder (4) with a 3.2 cm inside diameter, a 1.2 cm outside diameter, inner coaxial cylindrical center tube (5), a length adjustable sliding short (6), and an endplate (7) that is soldered to the outer cylinder (4). These cylindrical brass conducting pieces [(4)–(7)] form a continuous, adjustable conducting path within the excitation region.

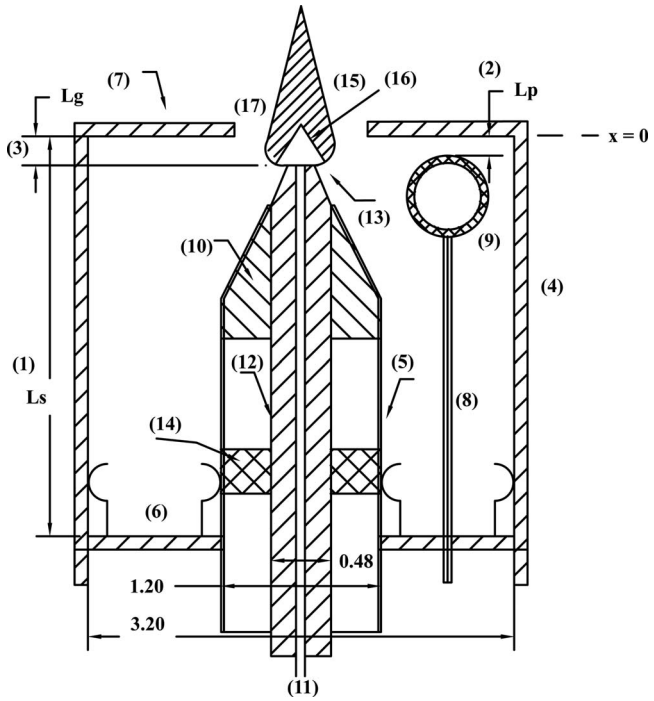

FIG. 4. The cross-section of the microwave re-entrant coaxial cavity applicator.

Thus, the cavity applicator is a variable length coaxial transmission line that is short circuited at one end. In the absence of a flame it has a capacitive gap at the other end.

Microwave energy is coupled into the cavity via a microcoaxial cable (8), which is terminated with a coupling loop (9). The input coupling cable (8) and loop (9) can be adjusted for optimal coupling by varying the position L_p (2) and its orientation (phi, ϕ). A brass nozzle plug (10) is inserted into the end of the center conductor (5). The brass nozzle has top circular surface of 4.8 mm in diameter with a tapered section 0.7 cm in length extending from the top surface to the opening of the center conductor (5). The brass nozzle is press fitted into the inner conductor (5). The gap length L_g (3) can be varied by ±5 mm above and below the $x=0$ reference plane shown in Fig. 4 by varying the independently adjustable center conductor (5). Input feed gases flow through a brass tube (11) located inside the inner conductor (12), which is coaxially placed inside the center conductor (5). Combustion gases, oxygen and methane, exit through a 0.4 mm diameter orifice (13) into the cavity capacitive gap region. A Teflon spacer (14) is placed between the center conductor (5) and inner brass tube (12) to provide support for the gas feed and water cooling systems. The brass tube (12) is water cooled (water cooling is not shown in Fig. 4) in order to prevent the plug (10) from overheating during microwave energy interaction with the flame. The premixed flame (15) and its inner cone (16) are located at the end of the nozzle. A 1 cm diameter circular hole (17) at the end plate enables the gases and the flame to exhaust and extend out of the cavity applicator.

In the experiments reported here, the cavity applicator is excited with 2.45 GHz energy, and the applicator is excited in the TEM coaxial wave mode. The cutoff frequency of the next lowest mode for the coaxial waveguide, i.e., the TE_{11} mode, is 5.4 GHz; hence only the TEM mode can be excited in the coaxial section of the cavity. The wavelength λ for the TEM mode is the free space wavelength and is ~12.24 cm at 2.45 GHz. The cavity quality factor Q is a measure of the electromagnetic energy loss per cycle of the resonant applicator. Lower loss implies a higher Q. The empty nonflame cavity Q depends on the condition of the cavity walls, sliding short, etc. and varies between approximately 500 and 1000. When the applicator is adjusted with a small gap, the length of L_s for resonance is approximately less than a quarter wavelength. As is shown in Fig. 5 the microwave energy is concentrated around the "gap region" at the end of the nozzle where the flame is located. This plot is obtained numerically using "rf electromagnetic solver" module of COMSOL MULTIPHYSICS computer program. The electromagnetic waves solver allowed us to visually predict the electric field distribution within the coaxial cavity structure. In Fig. 5 the relative electric field strength is indicated by the length of the arrows. When the applicator is adjusted for resonance the electric field intensity is the highest in the gap region. When the cavity is empty, i.e., when the flame is not ignited, the cavity can be adjusted by tuning the gap length L_g and the sliding short position L_s to a critically coupled resonance. Then the applicator is matched to the external 2.45 GHz power supply. This impedance matching increases the microwave electric field intensity in the gap region. When the applicator is matched the gap electric field can also be varied by changing the input power. The applicator has a very small excitation volume, and given a specific input power it operates with a large impressed electromagnetic power density.

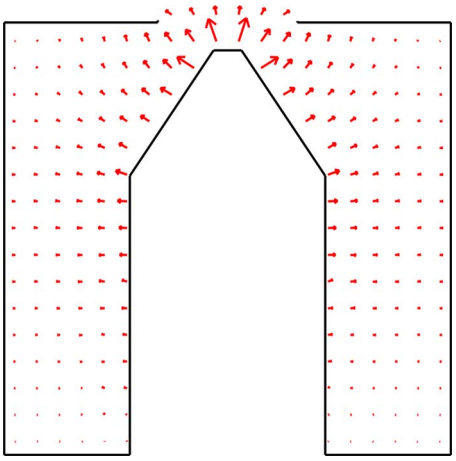

FIG. 5. (Color online) Numerically calculated relative electric field distributions inside the coaxial applicator with no flame/discharge present. The lengths of the arrows indicate the relative magnitude of the electric field strength. Frequency=2.45 GHz, cavity ID=3.2 cm, L_s=3.1 cm, inner conductor OD=1.2 cm, and L_g=2 mm.

The tuning adjustments and the microwave matching of this cavity have already been demonstrated with both low and high power microwave excitation levels in microwave discharge applications.[20,22] As the flame loading changes due to changes in input gas flow rates, gas mixtures, and variations in the input power, the applicator must be slightly retuned to achieve an efficient matched operating condition. The tuning adjustments that are necessary for matching the microwave energy into the cavity are (1) gap length L_g, (2) sliding short length L_s, (3) coupling loop length L_p, and (4) ϕ positions. All tuning variables, i.e., L_g, L_s, L_p, and loop orientation ϕ, are continuously variable. Typical experimental operating positions are L_g=0.1 cm, L_s=2.8 cm, L_p =0.2 cm, and ϕ=180° (i.e., the loop lies in the plane of Fig. 4).

B. The equivalent circuit of the applicator

In order to understand the coupling between the flame and the microwave energy we developed an equivalent circuit model of the applicator system. Figure 6 displays such

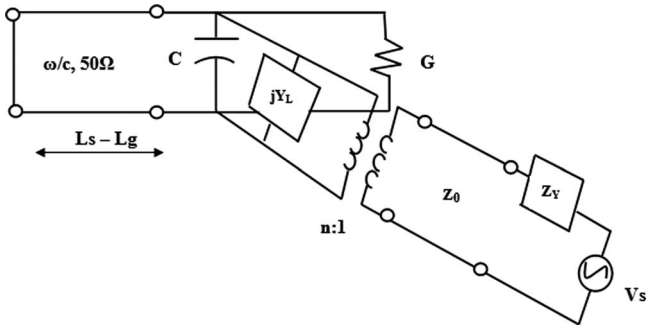

FIG. 6. Equivalent circuit of the microwave re-entrant cavity applicator.

an equivalent applicator circuit. For simplicity the microwave losses due to the surface currents on the coupling loop and the application are neglected. The circuit consists of a variable length $(L_s - L_g)$, 50 Ω transmission line, which extends from the sliding short to the gap region, the coupling loop circuit, and the gap circuit. The impedance of the shorted transmission line is given by $Z_{sc} = j50 \tan \beta_0 (L_s - L_g) = jX_{line}$, where Z_{sc} is the input impedance of the shorted line, $Z_0 = 50$ is the characteristic impedance of the coaxial applicator, $(L_s - L_g)$ is the length of the transmission line, and β_0 is the propagation constant of the line and is equal to $2\pi/\lambda$, where λ is the free space wavelength.

The coupling loop is modeled as an ideal transformer with an $n:1$ turns ratio and the lumped circuit reactance jY_L. This reactance represents the stored energy of evanescent fields associated with the near electric field of the loop. The coupling loop circuit is connected to the microwave power generator and the external microwave power measurement system. These external circuits are shown in Fig. 6 as an equivalent transmission line with a characteristic impedance of Z_0. This transmission line is connected to the microwave power supply and is modeled as an internal impedance of Z_Y (Z_0 is approximately equal to Z_Y) and an equivalent ideal voltage source V_s. The gap region is modeled as an equivalent circuit consisting of a lumped capacitor C and resistor G, which are connected in parallel with each other and with the sliding short transmission line and the input coupling circuit. The capacitance is the equivalent lumped circuit capacitance C that is produced by the strong electric fields that exist at the end of the applicator between the center conductor nozzle plug (10) and the endplate (7) (see Fig. 4). When there is no flame present, we assume for simplicity that the gap conductance is infinite, i.e., $G = \infty$, neglecting the microwave losses due to the surface currents on (7) and (10). Then, for simplicity the gap is modeled as an equivalent parallel plate capacitance that is given by

$$C = \frac{\varepsilon_0 A_{\text{eff}}}{L_g}, \tag{1}$$

where A_{eff} is defined as the equivalent effective parallel plate area of the gap region and L_g is the gap spacing referred to the $x=0$ plane. When the gap length is varied, A_{eff} also changes.

When the flame is ignited, the gap capacitance is further modified by the presence of the hot neutral gases and the low-density electron and ion gases produced by combustion. Microwave energy is introduced into the applicator by adjusting the applicator to an electromagnetic resonance at the 2.45 GHz excitation frequency, and then the microwave energy is coupled into the flame via Ohmic heating of the flame electron gas. The flame loaded gap impedance then becomes complex and has a real part represented by the conductance G and an equivalent effective gap capacitance C shown in Fig. 6. The conductance G represents the equivalent resistance produced by the Ohmic heating losses due to the coupling between the microwave energy and the flame electron gas, and the gap capacitance can be modeled as equivalent plasma filled capacitor (see as an example of such a capacitor in Ref. 29). As the impressed microwave power increases the densities of the electron and ion gases in the flame increase due to increased inelastic collision processes. The effective gap impedance is expected to be further changed by the presence of these higher charge densities and the Ohmic heating losses and at the higher input microwave power levels also due to the formation of microdischarges between the edge surfaces of (7) and (10) in Fig. 4.

At resonance, jY_L is usually much larger than the admittance of the gap and usually can be neglected. When the applicator is adjusted for resonance the capacitive reactance of the flame and plasma loaded gap must be canceled by the inductive reactance of the short-circuited transmission line. This can be expressed mathematically as

$$jX_{\text{gap}} + jX_{\text{line}} = 0, \tag{2}$$

where jX_{gap} is the effective capacitive reactance of the gap and jX_{line} is the reactance of the short-circuited transmission line. The capacitive reactance of the gap region is given by

$$jX_{\text{gap}} = \frac{1}{j\omega C} = \frac{-j}{\omega C}. \tag{3}$$

Thus Eq. (2) becomes

$$jX_{\text{gap}} = -jX_{\text{line}} = -j50 \tan \beta_0 (L_s - L_g), \tag{4}$$

where $\beta_0 = \omega/c$ and c is the speed of light. Noting that $L_s \gg L_g$ and solving for L_s yield

$$\beta_0 L_s \leq \tan^{-1}\left(\frac{1}{50\omega C}\right). \tag{5}$$

If C is small we have $\beta_0 L_s = \pi/2$ and $L_s = \lambda/4$, and then for all C, as C increases, the line resonant length becomes shorter. Thus,

$$L_s \leq \frac{2\pi/\beta_0}{4} < \left(\frac{\lambda}{4} \approx 3.1 \text{ cm}\right). \tag{6}$$

This result indicates that the resonant length L_s is less than a quarter wavelength and varies with the gap reactance. The experimentally observed lengths L_s vary from 1.9 to 2.8 cm depending on the gap size and the flame and microplasma loading. As the loading varies due to the changes in the chemistry, flow rate, or microwave input power, the applicator length L_s and/or the gap length L_g must be slightly varied to achieve optimal coupling and a microwave matched applicator.

C. The external microwave circuit and gas handling systems

Figure 7 displays the external microwave circuit. All experiments were performed in open air at atmospheric pressure. The microwave oscillator is a 2.45 GHz, continuously variable 0–100 W power supply. It is connected to one port of a three-port circulator via a 50 dB directional coupler, which measures the incident power P_{inc}. Another port of the circulator is connected to a 30 dB directional coupler, which measures the reflected power P_{ref}. This 30 dB directional coupler is connected to a matched load, which absorbs any reflected signal from the transmission mismatch. Thus input power absorbed by the applicator and the flame is $P_{\text{abs}} = P_{\text{inc}} - P_{\text{ref}}$. All of the microwave circuit components are

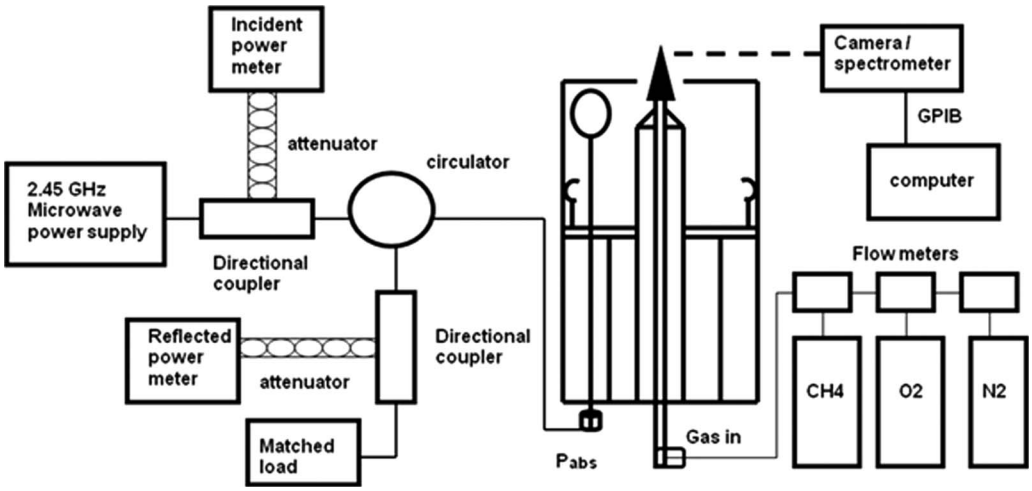

FIG. 7. Experimental setup for the microwave applicator combustion system operating in air at atmospheric pressure.

connected by 50 Ω, low power flexible coaxial cables. The cross-sectional view of the microwave applicator and the input gases handling system is also shown in Fig. 7. The gas handling system consists of flow meters and gas bottles for methane, oxygen, nitrogen, and argon. The premixed gas, which is regulated by the mass flow controllers, flows through the inner conductor of the applicator from gas feed tanks. A digital camera and/or spectrometer capture the flame image and its emission intensity, respectively, outside the cavity applicator end plate.

III. RESULTS AND DISCUSSION

A. Influence of microwave coupling on the flame structure

Figure 8 displays the visual images of the plasma flame as the input microwave power levels were varied from 0 to 20 W. The CH_4/O_2 input gas flow rate was held constant at 49/98 SCCM (SCCM denotes standard cubic centimeter per minute at STP) as the input power was gradually increased from 0 to 20 W. As the input power is increased the length, width, and intensity of the flame also correspondingly increase, and the flame color also changes, suggesting a change in the combustion process due to the presence of different radicals. When subjected to the increasing microwave power, the length of the flame increases gradually from about 2 up to 10 mm. Even at the low input power levels of 3–8 W the flame size and intensity increase, suggesting that at these low input impressed power levels, microwave energy is coupled into the electron gas, which in turn transfers its energy into excited radicals. At the higher input power levels of 10–20 W the flame continues to increase in size and intensity, and the flame appears to have a strong interaction with the microwave input energy, resulting in additional ionization and in an increase in electron and ion densities; and under certain conditions microplasmas appear in the gap region between the edge conducting surfaces of (7) and (10) in Fig. 4. At microwave power levels greater than 15 W the power coupled into the applicator is approaching or is of the same order of magnitude as the combustion flame power, which is 29 W. Thus, at the higher power levels shown in Fig. 8 "hybrid flame" is produced. This behavior is similar to that reported earlier[18] in the larger cavity applicator except here; the changes in the flame occur with much lower input microwave power levels, and changes in the appearance of the flame are more gradual and continuous versus increases in input power. Clearly, the coupling of microwave power into the premixed flame changes the physical appearance of the flame, and the microwave energy coupling is more efficient, i.e., with only a few watts to 10 W instead of 30–50 W as reported earlier[18] with the larger, less efficient applicator system.

A closer view of the flame is displayed in the photos in Fig. 9. It was observed that as microwave input power is applied to the combustion flame, the intensity of the flame inner cone in the ignition zone increases, and the cone shifts slightly up stream as the input power increases. Furthermore, as observed in Fig. 8, as the input power increases, the size

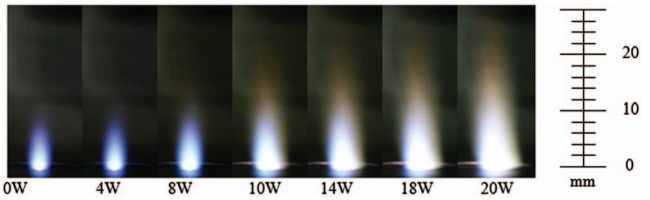

FIG. 8. (Color) Visual images of combustion flames as microwave power levels are varied from 0 to 20 W for flow rates of 49/98 SCCM CH_4/O_2. The gap length is $L_g=1$ mm below the $x=0$.

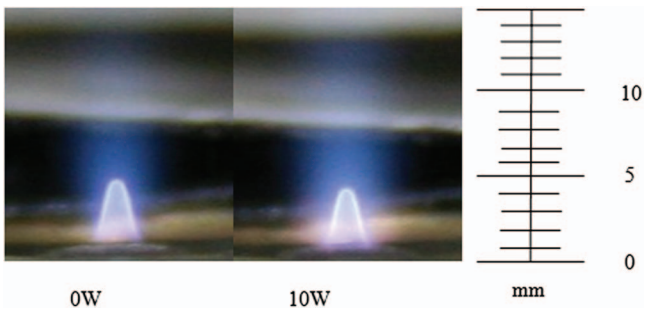

FIG. 9. (Color) Visual images of the inner cone premixed flame reaction zone with increasing microwave power at flow rates of 70/140 SCCM CH_4/O_2.

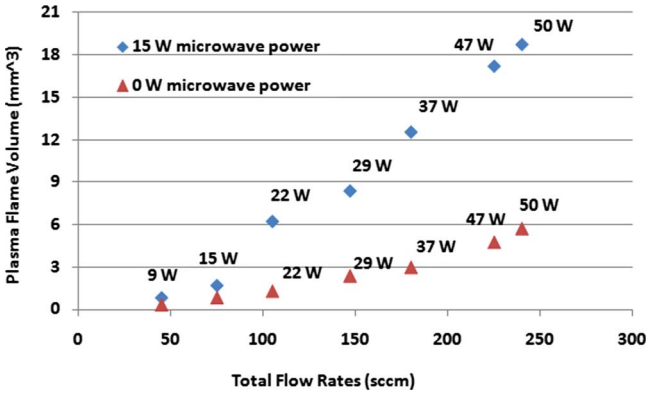

FIG. 10. (Color online) Plasma flame volume vs total flow rates at 0 and 15 W microwave power with its corresponding combustion flame power.

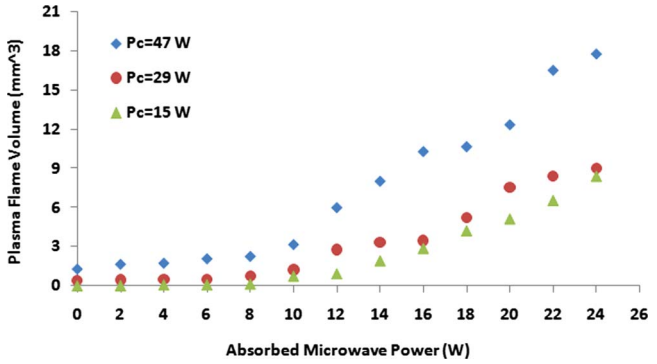

FIG. 11. (Color online) Plasma flame volume with increasing microwave energy at various total flow rates with its corresponding combustion power. P_c is the combustion power at each flow rate.

and intensity of the flame downstream "afterglow" increase. This suggests that as the microwave power is coupled into the flame the downstream, chemical activity and energy of the combustion flame increase. Also, microplasma formation is observed, which can be seen in the 10 W picture in Fig. 9 as an increased intensity, outer pink ring of excited species. Since the operation of the premixed flame is at atmospheric pressure, the plasma region in the flame is relatively thin, and the microwave heating of the electron gas takes place in or near the intense cone region of the flame. When the electrons are excited and heated their inelastic collision rates with the neutral gas molecules are increased, and electron and ion impact reactions can significantly impact the hydrogen chemistry of the fuel. In particular, it can lead to changes in the C_1 and C_2 chemistry and heat release channels involving CO and CO_2 conversion by introducing new and intermediate species and radical byproducts that result in a larger visual downstream flame volume. The appearance of yellowish color at the flame edge downstream at higher microwave power above 10 W (see Fig. 8) could be due to emission from alternative species, nitrogen entrainment, and changes in species concentration. This compact applicator design with the tapered coaxial inner conductor focuses a strong electric field onto the flame region located at the nozzle tip, enabling the efficient coupling of microwave energy into the flame.

Figure 10 displays the variation in flame volume versus flow rate without microwave power and with a constant 15 W of input microwave power. As shown the total flow rates are varied from 45 to 240 SCCM with a stoichiometric ratio of $CH_4/O_2=\frac{1}{2}$. The "flame volume" is calculated based on the brightest luminescence of the visual images that are obtained from photographic measurements. Two rulers are placed right by the combustion flame vertically and horizontally as a reference point to measuring the length and diameter of the flame. Then, the two dimensional images conical shape obtained from the camera photographs is quantified. The appearance of the afterglow and outer layer of the flame on the visual images was not taken into account for these volume calculations. The combustion power for each data point is approximated using the higher heating value for gaseous methane based on stoichiometric combustion.

As shown in Fig. 10 the flame volume increases for both combustion only (0 W) and also with the addition of 15 W of microwave power. These results are expected since higher total gas flow results in a larger diameter and a longer flame. The increase in flame volume with the application of microwave power suggests that the plasma is impacting the flow velocity prior to flame reaction and the increase in flame size past the reaction zone is an indication that the reaction itself is being energized. As shown in Fig. 10, as the microwave input power increases, the flame volume increases more dramatically when the total flow rates are higher as compared to the corresponding increases for lower total flow rates.

Figure 11 shows the variation in the flame volume for three flow rates versus absorbed microwave power. The three different flow rates of CH_4/O_2 are 75/150, 50/100, and 25/50 SCCM. As displayed visually in Fig. 8 and also as can be seen from the plot in Fig. 11, the volume of the flame increases as the microwave power varies from 0 to 25 W. Again, the higher total flow rates resulted in larger flame lengths and diameters.

B. Flammability limits

In terms of flammability limits, i.e., the limit of the flame to sustain itself in a fuel rich or fuel lean mixture ratio, the extension of the flame discharge to leaner burning operating conditions is shown Fig. 12. We conducted the blowout tests holding the oxygen flow constant and lowering the methane flow rate until the flame blew out. The x-axis of the graph represents the total flow rates of the fuel and oxidizer. The y-axis represents the equivalence ratio (ER), which is defined as the volume flow rate ratio of the experimental fuel/oxidizer divided by the fuel/oxidizer for stoichiometric burning of CH_4/O_2, which is 1/2.

$$\mathrm{ER} = (V_{\mathrm{CH_4}}/V_{\mathrm{O_2}})/(1/2), \tag{7}$$

where $V_{\mathrm{CH_4}}$ and $V_{\mathrm{O_2}}$ are the total flow rates of the fuel and oxidizer gas. The addition of 3 W of microwave power to the combustion flame can lower the ER compared to combustion only. The addition of 6 W or higher of microwave power allows operation at lean burning conditions to the point of zero fuel, i.e., ER=0.

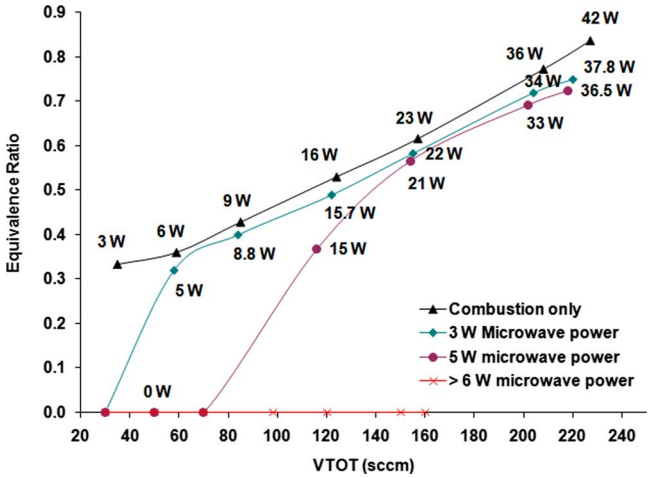

FIG. 12. (Color online) Flame extinction curves for combustion flames with 0, 3, 5, and 6 W additional of microwave power. The corresponding combustion power is displayed for each data point.

C. Optical emission spectroscopy measurements

Spectroscopic optical diagnostics on spectra intensity and gas temperature were performed. The CH radical species was used to determine the temperature of the plasma flame. The rotational temperature of CH in the plasma flame was measured at various microwave power levels and different ERs. The calculation method employed was by using the relative intensity of the rotational lines associated with the system *I*, $A^2\Delta \rightarrow X^2\Pi$ (0,0) pure rotational electronic transitions with the chemiluminescene located near 430 nm. The spectroscopic measurements were conducted across a line of sight passing through the reaction zone, i.e., near the cone region on the centerline of the plasma flame in a core part of the flame a few millimeters above the nozzle orifice surface. The relative upper level energy and its associated constants for the rotational temperature calculation are used as described in Ref. 30.

Optical emission wide scans of combustion only and combustion with the addition of 10 W of microwave power into the combustion flame are depicted in Fig. 13. The emission spectra were scanned from 3000 to 6000 Å visible wavelength. Clearly, with 10 W addition of microwave absorbed power to a flame with a combustion power of 29 W, the intensity of the spectra increases dramatically compared to combustion only. This clearly indicates that the microwave energy input alters the combustion flame. The nitrogen electronic excitation and other molecules are also detected when microwave power is added into the combustion flame. Shown in Fig. 14 are the optical emission spectra for a nitrogen emission without and with the addition of microwave power from 3 to 10 W. The spectral intensities were increased with only 5 W of input microwave power. With the application of microwave energy, the excited flame front was altered and the number of excited states of species was increased.

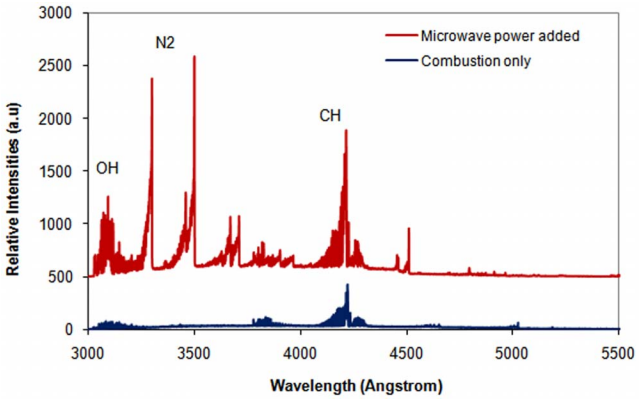

FIG. 13. (Color online) Optical emission spectroscopy spectra scan of combustion flames with and without addition of microwave power energy into the flame. Flow rates: 50/100 SCCM CH_4/O_2; microwave input power: 10 W.

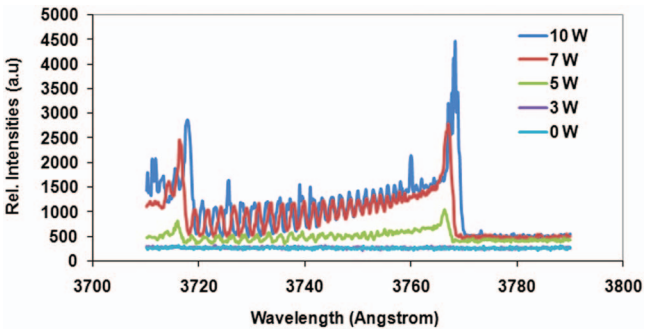

FIG. 14. (Color) Optical emission spectroscopy nitrogen line spectra of the plasma flame with 0, 3, 5, 7, and 10 W addition of microwave power into the combustion flame. Note that 0 and 3 W spectra are overlapping.

Figure 15 shows the CH rotational temperature of the hybrid plasma flame at various microwave power levels for three different flow rates, fuel lean (ER=0.6), ideal (ER=1.0), and fuel rich (ER=1.4). The measured rotational temperatures range from 2500 to 3600 K. The temperature increases as microwave power is added into the combustion flame. The influence of microwave power on the plasma flame temperature was more pronounced when operating at much leaner flames. Among the three different equivalent ratios, the highest temperature was obtained under fuel lean conditions.

D. Microwave energy and flame coupling mechanisms

As shown in Figs. 4 and 5, when the flame is ignited, the inner cone of the flame as well as some part of the down-

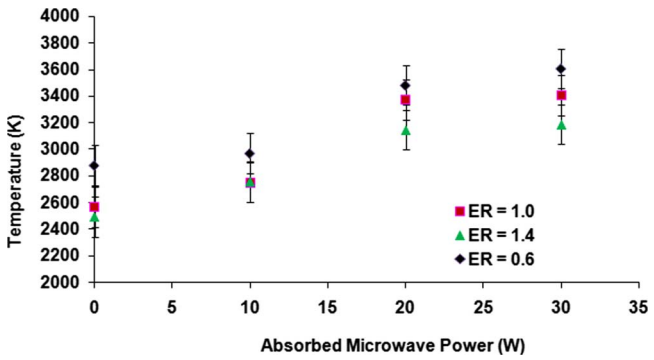

FIG. 15. (Color online) Plasma flame temperature as microwave power is added into the flame at three different equivalent ratios CH_4/O_2: 70/100, 50/100, and 25/100 SCCM. ER is the equivalent ratio that corresponds to flame fuel composition with ER=1.0 as the stoichiometric/ideal flame.

stream afterglow of the flame is located in the high electric field gap region of the applicator. Thus, any electron gas that exists within the flame due to combustion is also located in the high electric field region of the flame. It is expected that the combustion-produced electron gas is localized and will have densities much lower than the critical density ($<10^{11}/\mathrm{cm}^{-3}$ for 2.45 GHz excitation). Thus, the flame plasma is low-density plasma and the impressed microwave electric fields freely penetrate the electron gas to accelerate the electrons between collisions. In this atmospheric flame ($T_g=2500-3600$ K) the mean free path (MFP) for the electron molecule/radical collisions is of the order of 1 μm. The collision frequency for momentum transfer is of the order of $10^{11}/\mathrm{s}$. Thus the microwave electric field will heat the electron gas via elastic electron–neutral collisions, i.e., electron gas heating occurs by a collisional or Ohmic heating process that is governed by the following equation:

$$\langle P_{\mathrm{abs}}\rangle(\vec{r}) = \frac{1}{2}\frac{n_{\mathrm{oe}}(\vec{r})e^2}{2m_e\upsilon_m}\left(\frac{\upsilon_m{}^2}{\omega^2+\upsilon_m{}^2}\right)|\vec{E}(\vec{r})|^2, \tag{8}$$

where $\langle P_{\mathrm{abs}}\rangle(\vec{r})$ is the absorbed microwave power density in W/cm^3, $n_{\mathrm{oe}}(\vec{r})$ is the electron density in cm^{-3} versus position $\vec{r}$ in the electron gas, υ_m is the electron neutral collision frequency for momentum transfer, $\omega=2\pi f$ is the angular frequency, and $\vec{E}(\vec{r})$ is the impressed electric field strength. Typically for our gas temperatures and pressures, υ_m is in the order of $10-20\omega$.

When the microwave energy is coupled into the applicator/flame load, electron gas heating takes place, and the electron gas temperature T_e increases above the gas temperature T_g ($T_e>T_g$) creating a nonequilibrium plasma. As the microwave electric field and microwave power are increased the electron temperature will increase to the level where some electron–neutral collisions are inelastic. Through this inelastic collision process the microwave excited electron gas produces new radical and excited species. If electric field strengths and power levels are further increased, ionization collisions may also occur. When the impressed electric field strength is sufficient to cause breakdown, microplasmas can be produced in the region between the conducting surfaces of (7) and (10) in Fig. 4. Microwave electron gas heating is expected to occur in or very near the inner cone region of the flame. Since the MFPs for collision processes are very small (of the order of 1 μm), the radical and ionized species will also be produced in or directly adjacent downstream from the electron gas. As the excited neutral gas flows downstream the radical and excited species de-excite and recombine through three body collisions, thereby increasing the local gas temperature. The gas temperature of the downstream microwave excited flame is consequently expected to increase as the input microwave power is increased.

IV. DISCUSSION

A coaxial re-entrant cavity applicator has experimentally demonstrated the microwave energy excitation of a premixed flame. The applicator couples and focuses the microwave energy into a small gap region where the flame is positioned. The mechanical tuning of the applicator allows for the efficient matching of microwave power into the flame and also allows the optimal positioning of the flame with respect to the impressed electric field. We have demonstrated that by coupling microwave power of less than 10 W into the combustion-premixed flame, the flame intensity, length, volume, and temperature are altered, and as the power is increased from 10 to 20 W, microplasmas are produced in and adjacent to the flame. Microwave energy can be continuously coupled into the flame from a few watts to over 30 W, resulting in a range of hybrid flame behaviors. That is, at the very low input power level microwave energy may directly interact with the flame electron gas, and as the input power level is increased further inelastic processes become important, resulting in the formation of microplasmas. Additional experimental investigations are required to understand the details of these complex microwave energy/flame coupling interactions and also to understand the properties of the resulting hybrid flame.

This applicator system is more compact and has a higher microwave coupling efficiency than earlier microwave applicators that were used in microwave plasma-assisted combustion investigations.[17,18] Our initial experiments indicate that the applicator can be optimally matched to the external input transmission line and microwave oscillator circuit. Only a few watts of microwave power are necessary to modify the combustion process. Clearly, the applicator "tuning" and the improved microwave focus greatly enhance the microwave flame coupling efficiency. The applicator itself and the entire input waveguide system consist of coaxial waveguides and coaxial cables, yielding a compact overall microwave system. The applicator's inherent efficiency may allow it to be excited with compact low power solid-state microwave power supplies, thereby yielding a compact, portable overall hybrid microwave plasma combustion system. This applicator-coupling concept can be scaled up to larger burner sizes. Because of the coaxial structure it can be excited with lower frequencies (less than 1 GHz, even down to megahertz frequencies). It is expected that the many variants of this applicator will find uses in plasma-assisted combustion investigations related to improved combustion stability, improved ignition, pollution reduction, surface treatments, and material processing applications.

ACKNOWLEDGMENTS

This work is supported by Fraunhofer USA, Center for Coatings and Laser Applications and the Richard M. Hong Chaired Professorship.

[1] S. M. Lee, C. S. Park, M. S. Cha, and S. H. Chung, IEEE Trans. Plasma Sci. **33**, 1703 (2005).
[2] S. D. T. Axford, J. M. Goodings, and A. N. Hayhurst, Combust. Flame **114**, 294 (1998).
[3] N. Chintala, A. Bao, G. Lou, and I. V. Adamovich, Combust. Flame **144**, 744 (2006).
[4] L. Bromberg, D. R. Cohn, A. Rabinovich, and N. Alexeev, Int. J. Hydrogen Energy **24**, 1131 (1999).
[5] L. A. Rosocha, D. M. Coates, D. Platts, and S. Stange, Phys. Plasmas **11**, 2950 (2004).
[6] S. Stange, Y. Kim, V. Ferreri, L. A. Rosocha, and D. M. Coates, IEEE Trans. Plasma Sci. **33**, 316 (2005).

[7] M. S. Cha, S. M. Lee, K. T. Kim, and S. H. Chung, Combust. Flame **141**, 438 (2005).
[8] F. Wang, J. B. Liu, J. Sinibaldi, C. Brophy, A. Kuthi, C. Jiang, P. Ronney, and M. A. Gundersen, IEEE Trans. Plasma Sci. **33**, 844 (2005).
[9] S. M. Starikovskaia, J. Phys. D **39**, R265 (2006).
[10] M. A. V. Ward, J. Microwave Power **12**, 187 (1977).
[11] M. A. V. Ward, J. Microwave Power **14**, 241 (1979).
[12] C. S. MacLatchy, R. M. Clements, and P. R. Smy, Combust. Flame **45**, 161 (1982).
[13] E. G. Groff and M. K. Krage, Combust. Flame **56**, 293 (1984).
[14] S. F. Mertz, J. Asmussen, and M. C. Hawley, IEEE Trans. Plasma Sci. **2**, 297 (1974).
[15] A. I. Babaritskii, I. E. Baranov, and M. B. Bibikov, High Energy Chem. **38**, 407 (2004).
[16] S. B. Leonov and D. A. Yarantsev, AIAA 2006-563 (2006).
[17] S. H. Zaidi, E. Stickman, X. Qin, Z. Zhao, S. Macheret, Y. Ju, and R. B. Miles, AIAA 2006-1217 (2006).
[18] K. W. Hemawan, C. L. Romel, S. Zuo, I. S. Wichman, T. A. Grotjohn, and J. Asmussen, Appl. Phys. Lett. **89**, 141501 (2006).
[19] J. Asmussen, H. H. Lin, B. Manring, and R. Fritz, Rev. Sci. Instrum. **58**, 1477 (1987).
[20] R. M. Fredericks and J. Asmussen, J. Appl. Phys. **42**, 3647 (1971).
[21] J. Asmussen, T. A. Grotjohn, T. Schuelke, M. Becker, M. Yaran, D. King, S. Wicklein, and D. K. Reinhard, Appl. Phys. Lett. **93**, 031502 (2008).
[22] J. Rogers and J. Asmussen, IEEE Trans. Plasma Sci. **10**, 11 (1982).
[23] J. Asmussen, R. Mallavarpu, J. R. Hamann, and H. C. Park, Proc. IEEE **62**, 109 (1974).
[24] J. Root and J. Asmussen, Rev. Sci. Instrum. **56**, 1511 (1985).
[25] S. Whitehair, J. Asmussen, and S. Nakanishi, J. Propul. Power **3**, 136 (1987).
[26] L. Mahoney, M. Dahimene, and J. Asmussen, Rev. Sci. Instrum. **59**, 448 (1988).
[27] A. Kono, T. Sugryama, T. Goto, H. Furuhashi, and Y. Uchaid, Jpn. J. Appl. Phys., Part 2 **40**, L238 (2001).
[28] A. Kono, T. Shibata, and A. Aramaki, Jpn. J. Appl. Phys., Part 1 **45**, 940 (2006).
[29] M. A. Lieberman and A. J. Lichtenberg, *Principles of Plasma Discharges and Materials Processing* (Wiley, New York, 1994) p. 339.
[30] J. S. Kim and M. A. Cappelli, J. Appl. Phys. **84**, 4595 (1998).
[31] B. Ranganath and T. Echekki, Int. J. Heat Mass Transfer **49**, 5075 (2006).